

of the force volume data, and to H.-J. Butt (MPI-P) for helpful discussions. A.-S.D. and U.J. thank Prof. H.W. Spiess for his continued support.

Keywords: adhesion forces • chemical force microscopy • molecular packing • monolayers • self-assembly

- [1] a) C. D. Frisbie, L. F. Rozsnyai, A. Noy, M. S. Wrighton, C. M. Lieber, *Science* **1994**, *265*, 2071; b) A. Noy, C. D. Frisbie, L. F. Rozsnyai, M. S. Wrighton, C. M. Lieber, *J. Am. Chem. Soc.* **1995**, *117*, 7943; c) A. Noy, D. V. Vezenov, C. M. Lieber, *Annu. Rev. Mater. Sci.* **1997**, *27*, 381.
- [2] E. W. van der Vegte, G. Hadziioannou, *Langmuir* **1997**, *13*, 4357.
- [3] a) R. Mc Kendry, M.-E. Theoclitou, C. Abell, T. Rayment, *Langmuir* **1998**, *14*, 2846; b) R. McKendry, M.-E. Theoclitou, C. Abell, T. Rayment, *Jpn. J. Appl. Phys.* **1999**, *38*, 3901; c) P. Eaton, J. R. Smith, P. Graham, J. D. Smart, T. G. Nevell, J. Tsibouklis, *Langmuir* **2002**, *18*, 3387.
- [4] S. C. Clear, P. F. Nealey, *J. Coll. Interf. Sci.* **1999**, *213*, 238.
- [5] a) B. D. Beake, G. J. Leggett, *Phys. Chem. Chem. Phys.* **1999**, *1*, 3345; b) B. D. Beake, G. J. Leggett, *Langmuir* **2000**, *16*, 735.
- [6] A. Lio, D. H. Charych, M. Salmeron, *J. Phys. Chem. B* **1997**, *101*, 3800.
- [7] H. I. Kim, V. Boiadjev, J. E. Houston, X.-Y. Zhu, J. D. Kiely, *Tribol. Lett.* **2001**, *10*, 97.
- [8] C. E. H. Berger, K. O. van der Werf, R. P. H. Kooyman, B. G. de Grooth, J. Greve, *Langmuir* **1995**, *11*, 4188.
- [9] A. Ulman, *Chem. Rev.* **1996**, *96*, 1533.
- [10] a) A.-S. Duwez, B. Nysten, *Langmuir* **2001**, *17*, 8287; b) A.-S. Duwez, C. Poleunis, P. Bertrand, B. Nysten, *Langmuir* **2001**, *17*, 6351.
- [11] K. Bierbaum, M. Grunze, A. A. Baski, L. F. Chi, W. Schrepp, H. Fuchs, *Langmuir* **1995**, *11*, 2143.
- [12] M. Goldmann, J. V. Davidovits, P. Silberzan, *Thin Solid Films* **1998**, *327–329*, 166.
- [13] K. I. Imura, Y. Nakajima, T. Kato, *Thin Solid Films* **2000**, *379*, 230.
- [14] K. Bierbaum, M. Kinzler, Ch. Wöll, M. Grunze, G. Hähner, S. Heid, F. Effenberger, *Langmuir* **1995**, *11*, 512.
- [15] M. T. McDermott, J.-B. D. Green, M. D. Porter, *Langmuir* **1997**, *13*, 2504.
- [16] S. Lee, Y. S. Shon, R. Colorado, Jr., R. L. Guenard, T. R. Lee, S. S. Perry, *Langmuir* **2000**, *16*, 2220.
- [17] L. Li, Q. Yu, S. Jiang, *J. Phys. Chem. B.* **1999**, *103*, 8290.
- [18] R. M. Pashley, J. Israelachvili, *Colloids Surf.* **1981**, *2*, 169.
- [19] H. K. Christenson, P. M. Claesson, *Adv. Colloid Interface Sci.* **2001**, *91*, 391.
- [20] S. K. Sinniah, A. B. Steel, C. J. Miller, J. E. Reutt-Robey, *J. Am. Chem. Soc.* **1996**, *118*, 8925.
- [21] M. M. Walczak, C. K. Chung, S. M. Stole, C. A. Widrig, M. D. Porter, *J. Am. Chem. Soc.* **1991**, *113*, 2370.
- [22] T. Nakagawa, K. Ogawa, T. Kurumizawa, S. Ozaki, *Jpn. J. Appl. Phys.* **1993**, *32*, L294.
- [23] E. W. van der Vegte, A. Subbotin, G. Hadziioannou, P. R. Ashton, J. A. Preece, *Langmuir* **2000**, *16*, 3249.
- [24] K. L. Johnson, K. Kendall, A. D. Roberts, *Proc. R. Soc. London Ser. A* **1971**, *324*, 301.
- [25] H. Klein, W. Blanc, R. Pierrisnard, C. Fauquet, Ph. Dumas, *Eur. Phys. J. B* **2000**, *14*, 371.
- [26] M. Tortonese, M. Kirk, *Proc. SPIE Int. Soc. Opt. Eng.* **1997**, *3009*, 53.

Received: March 11, 2003 [F746]

Revised: May 23, 2003

The Case of the Disappearing Monolayer: Alkylsilane Monolayer Formation, Oxidation, and Subsequent Transparency to Scanning Tunneling Microscopy

Kevin S. Schneider,^[a] Thomas M. Owens,^[a] Daniel R. Fossnacht,^[a] Bradford G. Orr,^{*[b]} and Mark M. Banaszak Holl^{*[a]}

Chemisorption of alkylsilanes, RSiH_3 ($\text{R} = \text{hexyl, octyl, octadecyl}$), occurs via cleavage of the three Si-H bonds and subsequent formation of three Si-Au bonds.^[1] The resulting novel class of alkylsilane-based monolayers on $\text{Au}(111)$ has been characterized by X-ray photoemission spectroscopy (XPS) and reflection-absorption infrared spectroscopy (RAIRS). Variable energy XPS studies suggest alkylsilane coverage and orientation on $\text{Au}(111)$ is similar to that found for alkanethiol monolayers.^[2, 3] Oxidation of the chemisorbed alkylsilane monolayer generates two novel and surprising results: 1) upon oxidation, the resulting alkylsiloxane layer becomes transparent to scanning tunneling microscopy (STM) imaging and 2) the oxidative conditions induce the gold surface to return to the $23 \times \sqrt{3}$ surface reconstruction typical for clean gold surfaces.

Results and Discussion

An STM image of clean $\text{Au}(111)$ $23 \times \sqrt{3}$ is displayed in Figure 1 a. The image displays the parallel striped features of the $\text{Au}(111)$ $23 \times \sqrt{3}$ surface reconstruction.^[4–6] Exposure to a saturating dose of octylsilane in ultrahigh vacuum (UHV) dramatically alters the surface topography (Figure 1 b). The octylsilane monolayer surface is characterized by an interwoven pattern of elevated sinuous ridges surrounding small, depressed regions. Adjacent ridges frequently combine to form looped or knotted features. The ridges are $\approx 0.8 \text{ \AA}$ high, relative to the depressed regions. In addition, there are numerous interstitial island features 20–40 \AA in diameter with apparent heights of 2.5–3.0 \AA relative to the darkly contrasted regions. The apparent height of an island feature is equivalent to and indistinguishable from that of a single-step Au terrace. The percentage of the area covered by Au islands in Figure 1 b (6.5%) is consistent with the ejection of one to two atoms per (1×23) primitive unit cell.^[7] The presence of the islands indicates relaxation of the $23 \times \sqrt{3}$ surface reconstruction and is consistent with formation of $\text{Au}(111)$ 1×1 .^[7, 8]

[a] Prof. M. M. Banaszak Holl, Dr. K. S. Schneider, T. M. Owens, D. R. Fossnacht
Department of Chemistry, University of Michigan
930 N. University, Ann Arbor, MI 48109-1055
Fax: (+1) 734-763-2307
E-mail: mbanasza@umich.edu

[b] Prof. B. G. Orr
Department of Physics, University of Michigan
500 E. University, Ann Arbor, MI 48109-1120
Fax: (+1) 734-764-2193
E-mail: orr@umich.edu

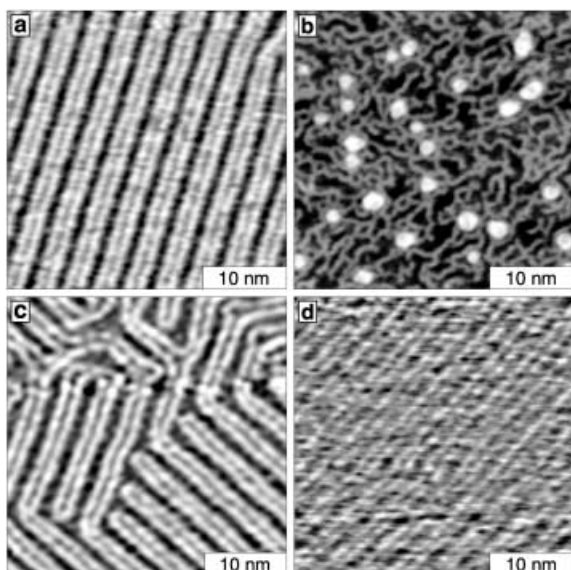


Figure 1. UHV-STM images of the same Au(111) sample (different sample areas), following successive experimental steps. All images are $35 \text{ nm} \times 35 \text{ nm}$. a) Clean Au(111) $23 \times \sqrt{3}$; sample bias (V_s) = -0.99 V , tunneling current (I_T) = 204 pA . b) Chemisorbed octylsilane monolayer formed on (a) following exposure to 50 L ($L = \text{langmuir} = 1 \times 10^{-6} \text{ torr} \cdot \text{s}$) gaseous octylsilane in UHV; $V_s = -1.00 \text{ V}$, $I_T = 262 \text{ pA}$. c) Oxidized physisorbed alkylsiloxane monolayer formed following exposure of (b) to ambient atmosphere for 15 min ; $V_s = 0.51 \text{ V}$, $I_T = 172 \text{ pA}$. d) Oxidized physisorbed alkylsiloxane monolayer in (c) following exposure to 50 L gaseous octylsilane in UHV; $V_s = 0.53 \text{ V}$, $I_T = 201 \text{ pA}$.

After adsorption of octylsilane, monoatomic terrace step edges are no longer smooth, which indicates Au migration to the edges upon relaxation of the reconstruction.

The origin of the sinuous ridges is not well understood. Arguments incorporating variations in alkyl chain orientation or angle have previously been employed to explain similar features for adsorbed alkanethiol species.^[9–11] The appearance of “striped” phases in alkanethiol monolayers is typically attributed to chain–chain interactions and/or crystallization. However, chemisorption of methanethiol (CH_3SH) onto Au(111) $23 \times \sqrt{3}$ also produces monolayer domains that exhibit a striped phase.^[12] Considering that the methanethiol monolayer lacks alkyl chains, the STM data suggest Au–S interactions may determine the alkanethiol monolayer features. Similarly, Au–Si interactions may dominate the structural features of the octylsilane monolayer shown in Figure 1 b.

Exposure to ambient atmosphere results in the disappearance of monolayer features from the STM image (Figure 1 c). The resulting surface is indistinguishable from clean Au(111) $23 \times \sqrt{3}$ (having identical lateral and vertical dimensions) under the imaging conditions employed, excepting the continued presence of roughened step edges. STM image features of the exposed monolayer do not vary with changes in tunneling current ($0.01 - 2 \text{ nA}$) or applied sample bias ($\pm 2 \text{ V}$). Occasionally, scanning probe microscopes “sweep” aside adsorbate layers to expose the underlying substrate.^[13] However, large area images ($500 \text{ nm} \times 500 \text{ nm}$) containing previously imaged smaller regions display no evidence of this behavior for these layers. In all instances, the images resemble clean Au(111) $23 \times \sqrt{3}$ terraces.

Exposure to additional octylsilane does not regenerate the image shown in Figure 1 b. Instead, an image identical to clean Au(111) $23 \times \sqrt{3}$ remains (Figure 1 d, degradation of image resolution is attributed to STM tip instability). The “clean gold” surface displayed in Figure 1 c does not have chemical properties identical to the authentic clean gold surface illustrated in Figure 1 a. Direct chemical analysis of oxidized sample surfaces using XPS has been performed to address this issue.

XPS spectra correlating to the surfaces in Figure 1 b and Figure 1 c are provided in Figure 2 a, 2 c and Figure 2 b, 2 d, respectively. Following exposure to ambient atmosphere, the Si 2p core level shifts by 2.3 eV to higher binding energy and the peak full width at half-maximum (fwhm) increases (Figure 2 b). The binding energy shift and peak broadening are consistent

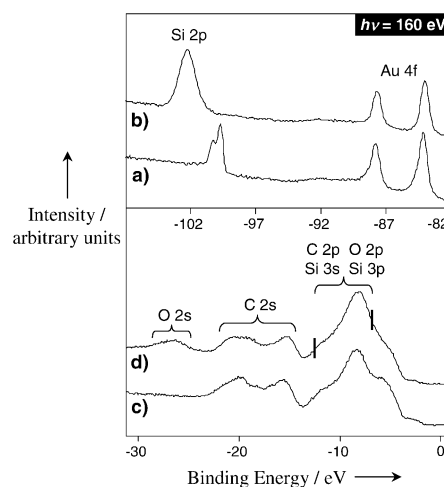


Figure 2. Soft X-ray photoemission spectra. a) Si 2p and Au 4f core level spectrum of an octylsilane monolayer on Au(111) formed from exposure to 440 L gaseous octylsilane in UHV. b) Si 2p and Au 4f core-level spectrum of the monolayer in (a), following exposure to ambient atmosphere for 15 min . c) Valence-band spectrum of the octylsilane monolayer on Au(111). d) Valence-band spectrum of the octylsilane monolayer in (c) following exposure to ambient atmosphere for 15 min .

with formation of a cross-linked RSiO_3 and/or $(\text{ROSiO}_{1.5})_n$ network. The features arising from the octyl chain are retained in the valence band (-12 to -20 eV), which indicates the presence of intact alkyl chains in the oxidized monolayer (Figure 2 d). In summary, the XPS data indicate that exposure to ambient atmosphere effectively oxidizes the silicon head-groups; however, all of the silicon and alkyl chains are retained within the oxidized monolayer. Thus, the STM image displayed in Figure 1 c does indeed have the monolayer present, albeit in an oxidized form.

Valence-band XPS data show the electronic states associated with the alkylsiloxane adlayer lie significantly below the gold Fermi level. Alkyl chain 2s states are $\approx 13 \text{ eV}$ lower in energy than the Fermi level and alkyl chain 2p and siloxane head group O 2p, Si 3s, and Si 3p states are $\approx 6 \text{ eV}$ lower in energy. Although this substantial difference in energy could reasonably make these states inaccessible for tunneling by STM, the energy difference is similar for both the alkylsilane and alkylsiloxane layers. The XPS

spectra show the gold Fermi levels are invariant, thus the Au(111) surface reconstruction does not substantially shift the energy of the gold states. This leaves two plausible explanations for the images displayed in Figure 1. It is possible that the orbitals associated with the Au(111) $23 \times \sqrt{3}$ reconstruction have a greater radial extent than those associated with Au(111) 1×1 . This could give rise to preferential tunneling into the gold surface orbitals, which effectively makes the alkylsiloxane layer "transparent". Alternatively, the original octylsilane monolayer image in Figure 1 b may simply be the result of significant mixing of Au and Si states. Oxidation of the Si head-groups removes this interaction, leaving only the Au states to image. In this case, the alkyl chains are "transparent" in both Figure 1 b and 1 c and it is only the Au–Si interaction that changes upon oxidation.

Scanning tunneling spectroscopy (STS) measurements of clean Au (\diamond), the octylsilane monolayer (\circ), and the oxidized monolayer (\square) are presented in Figure 3. The current versus

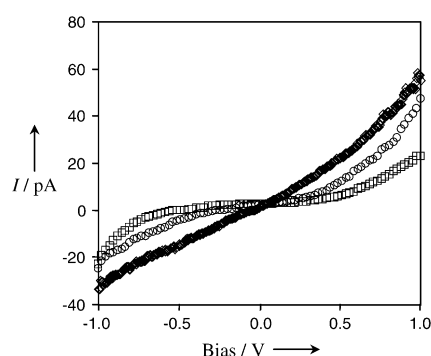


Figure 3. Scanning tunneling spectroscopy I – V curves of clean Au (\diamond), the octylsilane monolayer (\circ), and the oxidized octylsilane monolayer (\square).

voltage (I – V) curve for clean Au displays a linear ohmic relationship, expected for a conducting metallic substrate. However, the I – V curves of both the octylsilane and alkylsiloxane monolayers are decidedly nonlinear and clearly different from that of clean Au. Whereas STM imaging is only able to detect the presence of the octylsilane monolayer, STS can detect the presence of both the alkylsilane and transparent alkylsiloxane monolayers.

Summary

Oxidation of a chemisorbed alkylsilane monolayer on gold spontaneously regenerates the $23 \times \sqrt{3}$ surface reconstruction typical for clean gold surfaces. A protective alkylsiloxane layer remains on the surface, preventing further reactions with alkylsilane. The resulting alkylsiloxane monolayer is transparent to typical STM imaging conditions; however, STS can detect the presence of the layer. These observations indicate that STM studies of noble metal surfaces performed in oxidizing environments such as ambient atmosphere must be interpreted with caution. Chemisorbed species can oxidize, interact with the underlying metal surface as physisorbed layers, and give rise to

STM images that would typically be interpreted as clean metal surfaces.

Experimental Section

Au(111) samples for STM imaging experiments were prepared by annealing a commercially fabricated sample of Au deposited on mica (Molecular Imaging) to ≈ 673 – 773 K in UHV. In a separate chamber, ≈ 2500 Å gold (99.999%, Cerac, Inc) was deposited on the surface at ≈ 1 Å s^{-1} . Following Au deposition, the sample was further annealed (typically 3 h). Prior to octylsilane exposure, Au samples were imaged by STM in UHV to gauge overall sample cleanliness and confirm the presence of the Au(111) $23 \times \sqrt{3}$ surface reconstruction. Samples for XPS experiments consisted of Si wafers onto which a thin Cr layer was evaporated, followed by ≈ 1500 Å of Au. A fresh Au layer was evaporated in vacuo and sample cleanliness was assessed by XPS prior to octylsilane exposure.

n-Octylsilane ($\text{CH}_3(\text{CH}_2)_7\text{SiH}_3$) was purchased from Gelest, Inc. and loaded into a glass UHV-compatible container. Prior to experimental use, the sample was further purified by multiple freeze–pump–thaw cycles. Octylsilane was introduced into the UHV chambers via a leak valve at dosing pressures between 1×10^{-8} torr and 1×10^{-6} torr. Ambient exposure was achieved by removing the sample from UHV for 15 min. All chemical reactions and experimental characterization techniques were performed at room temperature. UHV–STM images were acquired in a previously described system.^[14] Low pass filters were employed to attenuate extraneous noise in the STM images. XPS was performed at beamline U8B at the National Synchrotron Light Source (NSLS) using monochromatic light. The beamline and endstation have been previously described.^[15] An incident photon energy of 160 eV was employed. Spectra were referenced to the binding energy of the Au $4f_{7/2}$ core level at 84.0 eV.

Acknowledgements

Dow Corning, RHK Technology, Inc. and the NSF (DMR-0093641 and INT-0096583) are thanked for their support. Research carried out in part at the National Synchrotron Light Source, Brookhaven National Laboratory, which is supported by the U.S. Department of Energy (Division of Materials Science and Division of Chemical Sciences of the Office of Basic Energy Sciences) under Contract No. DE-AC02–98CH10886. K.S.S. and D.R.F. thank the NSF for IGERT fellowships.

Keywords: chemisorption · monolayers · physisorption · scanning probe microscopy · X-ray photoelectron spectroscopy

- [1] T. M. Owens, K. T. Nicholson, M. M. Banaszak Holl, S. Süzer, *J. Am. Chem. Soc.* **2002**, *124*, 6800–6801.
- [2] C. D. Bain, G. M. Whitesides, *J. Phys. Chem.* **1989**, *93*, 1670–1673.
- [3] T. M. Owens, S. Süzer, M. M. Banaszak Holl, *J. Phys. Chem. B* **2003**, *107*, 3177–3182.
- [4] M. A. Van Hove, R. J. Koestner, P. C. Stair, J. P. Bibérian, L. L. Kresmodel, I. Bartoš, G. A. Somorjai, *Surf. Sci.* **1981**, *103*, 189–217.
- [5] U. Harten, A. M. Lahee, J. P. Toennies, C. Wöll, *Phys. Rev. Lett.* **1985**, *54*, 2619–2622.
- [6] C. Wöll, S. Chiang, R. J. Wilson, P. H. Lippel, *Phys. Rev. B* **1989**, *39*, 7988–7991.
- [7] G. E. Poirier, *Langmuir* **1997**, *13*, 2019–2026.

- [8] G. E. Poirier, E. D. Pylant, *Science* **1996**, *272*, 1145–1148.
[9] G. E. Poirier, M. J. Tarlov, *Langmuir* **1994**, *10*, 2853–2856.
[10] L. A. Bumm, J. J. Arnold, T. D. Dunbar, D. L. Allara, P. S. Weiss, *J. Phys. Chem. B* **1999**, *103*, 8122–8127.
[11] C. Zeng, B. Li, B. Wang, H. Wang, K. Wang, J. Yang, J. G. Hou, Q. Zhu, *J. Chem. Phys.* **2002**, *117*, 851–856.
[12] M. H. Dishner, J. C. Hemminger, F. J. Feher, *Langmuir* **1997**, *13*, 2318–2322.
[13] J. T. Woodward, M. L. Walker, C. W. Meuse, D. J. Vanderah, G. E. Poirier, A. L. Plant, *Langmuir* **2000**, *16*, 5347–5353.
[14] K. S. Schneider, K. T. Nicholson, D. R. Foshnacht, B. G. Orr, M. M. Banaszak Holl, *Langmuir* **2002**, *18*, 8116–8122.
[15] S. Lee, S. Makan, M. M. Banaszak Holl, F. R. McFeely, *J. Am. Chem. Soc.* **1994**, *116*, 11819–11826.

Received: May 22, 2003 [Z851]

Assembling Nanometer Nickel Particles into Ordered Arrays

Sheng-Bin Lei, Chen Wang,* Shu-Xia Yin, Li-Jun Wan, and Chun-Li Bai*^[a]

Introduction

Monolayer protected clusters (MPC) are considered to represent a new class of specimen due to their high stability in air and solvents, and also their derivatization flexibility.^[1] Although ligand-capped gold clusters have been known for a number of years, the practical formation of stable, isolable monolayer-protected clusters has only recently been demonstrated by Schiffrin and co-workers,^[2] and the preparation methodology was greatly advanced in the following years.^[3–7] In his seminal work, Schiffrin combined the classical two-phase colloid preparation of Faraday with contemporary phase transfer and alkanethiolate/Au chemistry to prepare very small clusters of gold. These alkanethiolate-protected MPCs differ from conventional colloids and nanoparticles in that they can be repeatedly isolated and redissolved in common organic solvents without irreversible aggregation. This property enables chemists to handle them with familiar procedures, including both isolation and surface reactions. The Schiffrin reaction can endure considerable modifications to protect both the ligand structures and the core metal of the MPCs. Reports of MPCs with Ag and alloy (Au/Ag, Au/Cu, Au/Ag/Cu, Au/Pt, Au/Pd, and Au/Ag/Cu/Pd) cores and various different structured ligands have appeared.^[8, 9]

Self-assembly from molecular-sized components is one promising approach for the construction of nanostructures. These components include organic molecules and monolayer-protected metal clusters. By the self-assembly approach, organic

molecules can form either two-dimensional ordered monolayers or one-dimensional molecular arrays.^[10, 11] For metal nanoparticles, 2D ordered monolayers have also been reported.^[12] Nanoparticle arrays assembled on a surface may exhibit electronic, optical, and sensor functions, and can be used to create a variety of electronic and sensor components.^[13] Herein, we report the synthesis and assembly of 1-dodecanethiol (C12SH)-capped nickel particles using an alkane-assembling monolayer as the template. It is well-known that alkane and alkane derivatives physisorbed on highly oriented pyrolytic graphite (HOPG) can form well-ordered monomolecular layers. The phenomena have been well-characterized by different techniques, such as scanning tunneling microscopy (STM) and electron scattering.^[14–18] Most alkane derivatives adsorb with their carbon chains parallel to the surface, and the functional groups paired together on the HOPG surface. Considering the different polarities and electronic properties of the functional groups from the alkane chains, this monolayer of alkane derivatives makes the surface of HOPG an ideal template for investigating the adsorption behavior of organic molecules. Compared with the nanofabricated surface,^[19] this alkane-derivative-modified surface is organic rather than metallic or semiconducting. The relative polarity and the ratio of the polar/nonpolar area could be modified easily, by changing the functional group and the chain length of the alkane derivative.

Assembling nanoparticles into ordered structures is one of the most interesting objects, because of its relevance to the construction of nanodevices and sensors. The current results demonstrate a possible means of obtaining an ordered array of nanoparticles using the template effect of an alkane monolayer, and will be helpful for reaching the goal of constructing nano-electronic devices.

Results and Discussion

2.1. STM Characterization of the Clusters

Figure 1 shows the image obtained by STM of the nanoparticles deposited on a graphite substrate. It can be observed on the STM image that the scale of particle diameter is in the range of 2 to 7 nm. Statistics of the particle diameters show that the average diameter is 3.2 nm. Since the diameter measured from the STM image is the outer diameter, which includes the monolayer of thiolate, and considering the approximate chain length of C12SH is 1.5 nm, the diameter of the nickel core is in the subnanometer to several nanometer range.

2.2. XRD, XPS, and UV Characterization

Usually, for transition metals like Fe, Co, or Ni reduced by NaBH₄, indirect investigation by X-ray diffraction (XRD) on an annealing powder has been reported as structural characterization. In the present case—as in data reported for similar experiments^[20, 21]—the XRD spectra had a broad peak (Figure 2a), which may correspond to the (111) diffraction. From the half-wave width of the diffraction peak, the average core diameter was calculated to be about 1.40 nm, consistent with that estimated from STM, and

[a] Prof. C. Wang, Prof. C.-L. Bai, Dr. S.-B. Lei, Dr. S.-X. Yin, Prof. L.-J. Wan
Center of Molecular Science, Institute of Chemistry
Chinese Academy of Sciences, Beijing, 100080 (China)
Fax: (+86) 10-62558934
E-mail: wangch@iccas.ac.cn, clbai@iccas.ac.cn